MATERIALE PLASTICE
https://revmaterialeplastice.ro
https://doi.org/10.37358/Mat.Plast.1964

High-Resolution DLP Printing of Elastic GelMA Hydrogel Scaffolds with Vascular-Mimetic Architecture for Microvascular Regeneration

XIAOTIAN ZHANG[1,#], KAI LI[1,#], SUYIN FENG[2,3*], RUNFENG SUN[1,2,4*], LI YANG[5*]

[1] Department of Cardiology, Donghai County People's Hospital (Affiliated Kangda College of Nanjing Medical University), Lianyungang, China
[2] Cardio-Cerebral Vascular Disease Prevention and Treatment Innovation Center, Donghai County People's Hospital (Affiliated Kangda College of Nanjing Medical University), Lianyungang, China
[3] Donghai Intelligent Medical Innovation Center, Kangda College of Nanjing Medical University, Lianyungang, China
[4] Jiangnan University Smart Healthcare Joint Laboratory, Donghai County People's Hospital (Affiliated Kangda College of Nanjing Medical University), Lianyungang, China
[5] Department of Cardiovascular Medicine, The Affiliated Zhuzhou Hospital Xiangya Medical College, Central South University, Zhuzhou, China

Abstract: ***Background:*** *The fabrication of vascular-mimetic hydrogel scaffolds with precise luminal geometry, suitable elasticity, and good cytocompatibility remains a major challenge in tissue engineering. Digital light processing (DLP) printing offers high resolution and rapid fabrication, but over-curing and limited structural fidelity in hollow constructs still restrict its application in vascular-like scaffold fabrication.* ***Methods:*** *In this study, GelMA-based tubular scaffolds with Y-shaped and curved vascular geometries were fabricated by DLP printing. To improve printing precision, 0.02% (w/v) tartrazine was introduced as a light-absorbing agent to regulate light penetration and curing depth during the photopolymerization process. The printed scaffolds were characterized by optical imaging and scanning electron microscopy, while their mechanical properties were evaluated through tensile and compression tests. Cytocompatibility was assessed using CCK-8 assay, Live/Dead staining, and quantitative cell survival analysis.* ***Results:*** *The incorporation of tartrazine effectively reduced excessive light penetration during printing, enabling the formation of continuous tubular structures with improved lumen definition and structural integrity. The DLP-printed GelMA scaffolds showed high geometric fidelity, with smooth and stable inner channels of approximately 1 mm in diameter. Mechanical testing demonstrated a nonlinear J-shaped tensile response and strain-stiffening behavior under compression, indicating favorable elasticity and resistance to deformation. In vitro biological evaluation further showed high cell viability, with CCK-8 results remaining above the control level and Live/Dead staining confirming a predominance of viable cells on the scaffold surface.* ***Conclusion:*** *The incorporation of a small amount of photoabsorber enabled high-resolution DLP printing of vascular-like GelMA scaffolds with excellent mechanical flexibility and biocompatibility. These constructs hold strong potential as perfusable, elastic hydrogel platforms for microvascular regeneration, endothelialization studies, and organ-on-chip applications.*

Keywords: *Microvascular regeneration, vascular-mimetic hydrogel scaffold, DLP printing, perfusable tissue constructs*

1. Introduction

The development of vascular-mimetic hydrogel scaffolds represents a critical step toward engineering functional tissue constructs that can integrate with native vasculature [1]. In natural tissues, hierarchical blood vessels distribute nutrients, oxygen, and biochemical signals throughout the entire

**email: fengsuyin@njmu.edu.cn; sunrunfeng_dh@njmu.edu.cn; qwyangli6463097@sina.com*
[#] These authors contributed equally to this work

structure, while also providing mechanical compliance and biological cues for cell organization [2]. Replicating such complexity in engineered scaffolds remains a major challenge, particularly the fabrication of perfusable, elastic, and biocompatible tubular architectures that can sustain physiological deformation and support cell adhesion under flow [3,4].

Three-dimensional (3D) printing technologies have recently emerged as powerful tools for constructing biomimetic hydrogels with high structural precision [5]. Among them, digital light processing (DLP) stands out due to its rapid fabrication speed, fine resolution, and ability to form smooth internal surfaces through layer-by-layer photopolymerization [6,7]. Unlike extrusion-based printing, which often causes filament fusion and surface roughness, DLP enables precise control over complex hollow geometries—an essential feature for vascular-like channels [8]. Nevertheless, several technical limitations remain, especially in the construction of hollow or vascular-like architectures. During photopolymerization, excessive light penetration and optical scattering may enlarge the effective curing region beyond the intended geometry, resulting in over-curing, reduced dimensional accuracy, and partial blockage or deformation of the lumen. These issues become more pronounced in photocurable hydrogel systems with high water content, where the balance between printability, structural fidelity, and biological compatibility is particularly difficult to maintain [9,10].

Gelatin methacryloyl (GelMA) has gained attention as an ideal photocurable biomaterial due to its tunable stiffness, mild crosslinking conditions, and intrinsic cell-adhesive motifs derived from gelatin [11]. For GelMA-based systems, this challenge of DLP printing is even more significant. Although GelMA is widely recognized for its excellent biocompatibility, tunable mechanical properties, and intrinsic cell-adhesive motifs, its use in DLP printing is often limited by insufficient control of curing depth and feature definition, especially when fabricating fine hollow channels or branched tubular structures. As a result, recent studies have increasingly emphasized the importance of regulating light transport within the prepolymer solution, for example by optimizing photoinitiator concentration, exposure conditions, or introducing light-absorbing additives to confine polymerization more precisely. These considerations define the technical starting point of the present study [12,13]. Incorporating a small amount of light absorber is an effective strategy to mitigate these problems. In this work, 0.02% (w/v) tartrazine was introduced as a photoabsorber to modulate the curing depth and enhance layer definition, enabling precise fabrication of perfusable GelMA scaffolds with smooth, continuous tubular channels [14].

This study aims to establish a DLP-based fabrication strategy for vascular-mimetic GelMA scaffolds that combine geometric accuracy, mechanical elasticity, and excellent cytocompatibility. Y-shaped and curved tubular structures were designed to mimic the branching morphology of native vessels. The mechanical performance of the printed scaffolds was systematically evaluated under tensile and compressive loading, and their biocompatibility was verified by CCK-8 and live/dead staining assays. Furthermore, a conceptual framework for microfluidic co-culture and organ-on-chip applications was proposed to highlight the potential of these scaffolds as perfusable, biomimetic hydrogel platforms for future microvascular regeneration and tissue–organ modeling.

2. Materials and methods

2.1. Materials

Gelatin methacryloyl (GelMA) was synthesized from type A porcine skin gelatin (Gelatin from porcine skin (gel strength ~300 Bloom, Type A; Sigma-Aldrich, St. Louis, MO, USA; G2500)) following a standard methacrylation protocol, yielding a degree of substitution of approximately 70%, as confirmed by ^{1}H NMR. Lithium phenyl-2,4,6-trimethylbenzoylphosphinate (LAP, Sigma-Aldrich, 900889) was used as the photoinitiator, and tartrazine (Sigma-Aldrich, T0388) served as a photoabsorber. All other reagents, including phosphate-buffered saline (PBS, without Ca^{2+}/Mg^{2+}), deionized water, and ethanol, were analytical grade.

Prepolymer ink formulation for DLP printing: GelMA (12% w/v) and LAP (0.25% w/v) were dissolved in PBS at 37°C under stirring, followed by addition of tartrazine (0.02% w/v, 0.2 mg mL^{-1}) as the photoabsorber. The solution was filtered through a 0.22 μm sterile membrane before printing. Tartrazine was used to limit light penetration and improve layer resolution, thereby ensuring accurate lumen formation and reducing over-curing in the inner channel.

2.2. CAD design and slicing

Y-shaped and curved tubular geometries were designed using SolidWorks with an internal diameter of 1.0 mm and wall thickness of 0.8–1.2 mm. Models were sliced into layers of 50 μm thickness, with medium anti-aliasing settings. No support structures were required for printing.

2.3. DLP printing parameters

Printing was performed on a 405 nm digital light processing (DLP) printer (e.g., Asiga MAX or Anycubic Photon) under ambient temperature (22–25°C).

- Light intensity: 5–10 mW cm^{-2} at the projection plane.
- Exposure settings:
  - Base layers (first 4): 10 s per layer
  - Normal layers: 1.5–2.0 s per layer
- *Z*-axis movement: lifting distance 3–5 mm, lifting/retracting speed 2–4 mm s^{-1}, resting time 0.5–1 s for resin recoating.

If inner-channel over-curing occurred, tartrazine concentration (0.015–0.025%) and exposure time (1.3–1.8 s) were fine-tuned to balance accuracy and interlayer bonding.

2.4. Post-processing

Printed scaffolds were rinsed gently in PBS twice (1 min each) to remove uncured resin. A secondary photocuring step was performed under a 405 nm light source for 2–5 min to ensure complete crosslinking. Samples were then immersed in 70% ethanol for 10 min, washed three times with PBS, and soaked overnight in PBS at 37°C (changing the buffer twice) to remove soluble residues prior to cell experiments.

2.5. Morphological characterization

Optical images were acquired using a stereomicroscope. Cross-sections were obtained by cryo-cutting or razor slicing. Samples were sputter-coated with a thin layer of gold (<5 nm) for SEM imaging (Hitachi SU8010). The inner diameter and wall thickness were analyzed by ImageJ at five random positions and expressed as mean ± SD.

2.6. Mechanical testing

Mechanical properties were measured using a universal testing machine (Instron 5943).

- Tensile test: rectangular GelMA strips (length = 20 mm, width = 5 mm, thickness = 1–2 mm) were stretched at a rate of 50 mm min^{-1} up to 100% strain.
- Compression test: cylindrical samples (Ø = 6–8 mm, height = 5–6 mm) were compressed at 10% strain min^{-1} to 80% deformation.

Engineering stress–strain curves were plotted, and the modulus and energy dissipation were extracted for comparison.

2.7. Cytocompatibility evaluation

Extract preparation: scaffolds were incubated in complete culture medium at 37°C for 24 h following ISO 10993-12 (surface-area-to-volume ratio: 3 cm^2 mL^{-1}).

CCK-8 assay: cells (5×10^3 cells/well) were seeded in 96-well plates, treated with scaffold extracts, and cultured for 0, 12, 24, 48, and 72 h. Absorbance at 450 nm was measured to evaluate cell viability relative to controls.

Live/Dead staining: cells seeded inside the tubular scaffolds were stained with Calcein-AM (2 μm) and EthD-1 (2 μm), rinsed with PBS, and imaged using confocal fluorescence microscopy. Cells adhered and spread along the inner wall, forming a vertical, band-like distribution.

2.8. Statistical analysis

All quantitative data are presented as mean ± SD (n ≥ 3). Statistical significance was determined using Student's *t*-test or one-way ANOVA, with $p < 0.05$ considered significant.

3. Results

As shown in Figure 1, the vascular-inspired design was successfully translated into 3D constructs using DLP printing. The process started from a CAD-based vascular model (Figure 1A), which guided the controlled photopolymerization of GelMA prepolymer into a defined elastic scaffold (Figure 1B). The printed constructs maintained high geometric fidelity, with smooth surface morphology and continuous lumen formation. The use of GelMA as an elastic hydrogel matrix provided sufficient mechanical flexibility for post-printing handling and potential perfusion applications (Figure 1C). The combination of biocompatible material composition and high-resolution light-based printing ensured both structural precision and cytocompatibility, laying the foundation for subsequent biological functionalization.

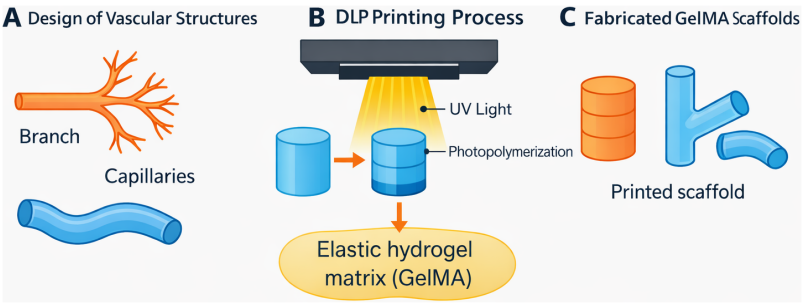

Figure 1. Schematic illustration of the design and fabrication of vascular-mimicking elastic hydrogel scaffolds via DLP printing

As shown in Figure 2, the CAD-modeled vascular geometries (Figure 2A) were accurately reproduced by the DLP printing process. The printed GelMA scaffolds (Figure 2B) exhibited clear Y-shaped and curved configurations consistent with the design, demonstrating the high resolution and dimensional stability of the system. The optical images revealed smooth surfaces and continuous lumen walls without defects or distortion. The SEM image (Figure 2C) confirmed that the printed channels maintained a uniform circular cross-section of approximately 1 mm in diameter, with a well-defined boundary between the lumen and the hydrogel matrix. The visible layer texture reflected the 50 μm printing resolution, indicating precise layer stacking and stable photopolymerization during fabrication.

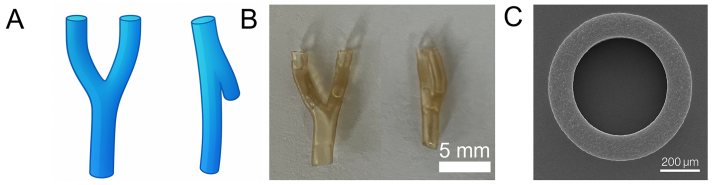

Figure 2. Morphological and structural characterization of DLP-printed GelMA vascular scaffolds. (A) CAD models of Y-shaped and curved vascular geometries used for printing. (B) Photographs of the corresponding printed GelMA scaffolds, showing good structural fidelity and continuous tubular morphology. (C) Cross-sectional SEM image of the printed tubular scaffold, revealing a well-defined circular lumen of approximately 1 mm in diameter and a layered wall microtexture characteristic of the DLP printing process

As illustrated in Figure 3A, the tensile test revealed a characteristic J-shaped stress–strain relationship, where the GelMA hydrogel exhibited low modulus at small deformations followed by rapid stiffening beyond 50% strain. This nonlinear elasticity mirrors the mechanical response of soft biological tissues such as blood vessels, enabling the scaffold to deform without permanent damage under physiological stretching. The ultimate tensile stress approached approximately 150–200 kPa at 100% elongation, confirming the excellent elasticity of the printed network.

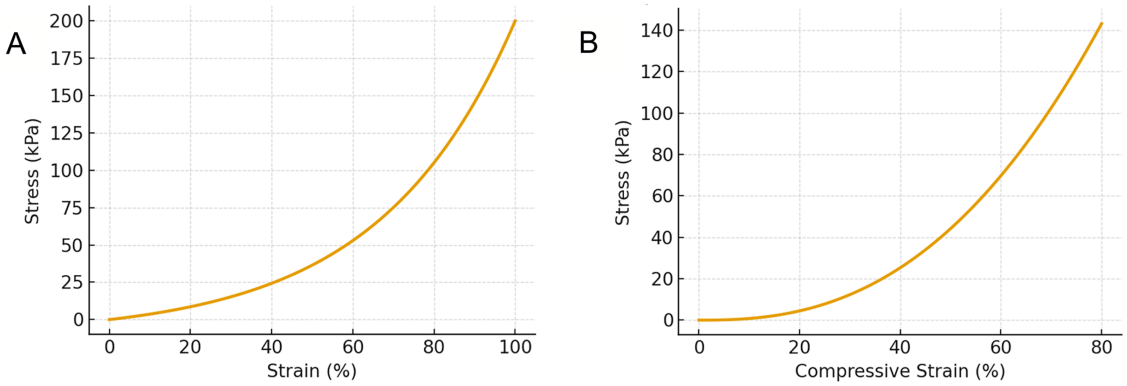

Figure 3. Mechanical characterization of the DLP-printed GelMA vascular scaffold. (A) Tensile stress–strain curve showing a typical nonlinear J-shaped response, with strain-induced stiffening at higher deformation. (B) Compression stress–strain curve showing a progressive increase in stress with strain, indicating good deformation resistance and structural stability under compression

Under compression (Figure 3B), the GelMA scaffold displayed a continuous increase in stress up to around 140 kPa at 80% strain. The curve exhibited a gradual slope at low strain and a pronounced hardening phase at higher strain levels, reflecting the densification of the hydrogel network and resistance to collapse. The absence of abrupt failure or structural discontinuity indicates that the printed constructs maintain integrity even under large compressive loads.

As shown in Figure 4A, the CCK-8 results demonstrated that the cells cultured on the DLP-printed GelMA scaffolds maintained high viability throughout the 72-h period. The viability gradually increased to approximately 108% relative to the control, indicating that the material and its photopolymerization residues did not induce cytotoxicity. Instead, a slight proliferation-promoting effect was observed, possibly due to the cell-adhesive properties of the GelMA matrix. In contrast, the control group maintained nearly constant viability, confirming the reliability of the assay.

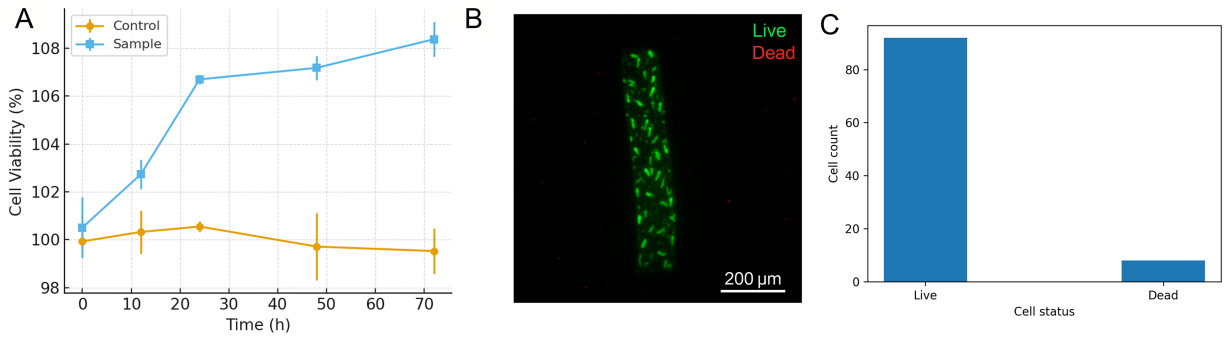

Figure 4. In vitro cytocompatibility assessment of the DLP-printed GelMA tubular scaffold. (A) CCK-8 assay showing the relative viability of cells cultured with the scaffold for up to 72 h. (B) Representative Live/Dead fluorescence image of cells on the tubular scaffold, with live cells shown in green and dead cells in red. (C) Quantitative analysis of the Live/Dead staining results, demonstrating a high proportion of viable cells, consistent with the CCK-8 assay

The live/dead staining results in Figure 4B further confirmed excellent cytocompatibility. Cells adhered uniformly along the inner wall of the printed tubular scaffold, forming a continuous cellular layer. Most of the cells exhibited green fluorescence (live), with only a few red-stained (dead) cells visible. The elongated morphology of the cells along the scaffold direction suggested a degree of alignment influenced by the curvature and confinement of the tubular geometry.

As conceptually illustrated in Figure 5A, the printed tubular GelMA scaffolds may serve as perfusable microenvironments for future microfluidic cell culture applications. Figure 5B presents a schematic comparison of the expected cellular morphology under static and fluid shear stress conditions, rather than direct experimental observations obtained in the present study. In addition, Figure 5C outlines the potential future use of these vascular-mimetic scaffolds in organ-on-chip platforms.

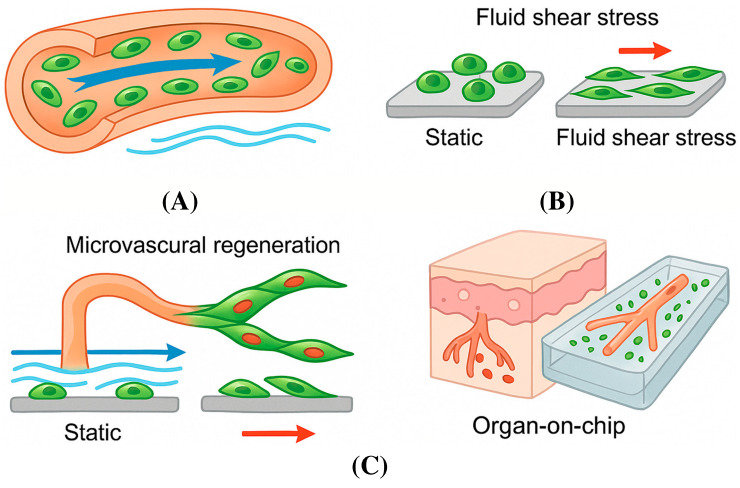

Figure 5. Conceptual illustration of the potential future applications of vascular-mimetic GelMA scaffolds. (A) Schematic representation of a possible microfluidic cell co-culture model based on perfusable tubular scaffolds. (B) Proposed comparison of cell morphology under static and fluid shear stress conditions. (C) Prospective applications of the printed scaffolds in organ-on-chip systems

4. Discussion

The schematic in Figure 1 highlights the feasibility of applying DLP printing to fabricate vascular-mimetic scaffolds with controllable elasticity and architecture. Compared with traditional extrusion-based bioprinting, the DLP technique offers superior spatial accuracy and smoother surface topography due to its photopolymerization-based voxel control [15]. The selected GelMA hydrogel provides a suitable compromise between printability and elasticity, enabling the formation of continuous lumen-like channels that can support fluid flow and potential endothelialization [16]. The branched geometries mimic the natural gradient from macrovessels to microcapillaries, which is crucial for achieving physiological flow resistance and nutrient transport. This figure thus establishes the conceptual and technical basis for constructing biofunctional, perfusable networks in future microvascular regeneration studies [17].

The successful fabrication of both Y-shaped and curved tubular scaffolds demonstrated that the present DLP-based strategy was capable of reproducing vascular-like architectures with relatively high geometric fidelity. In particular, the optical images and SEM observations confirmed that the printed constructs maintained continuous luminal structures and well-defined circular cross-sections, indicating that the printing parameters and resin formulation used in this study were sufficient to support stable hollow-structure formation. This result is especially important for vascular-mimetic scaffolds, because the integrity and continuity of the lumen directly determine the feasibility of later perfusion, cell seeding, and nutrient transport. Rather than merely obtaining a tubular shape, our results suggest that the present system can preserve the essential structural features required for mimicking simplified vascular pathways.

The results in Figure 2 verify the feasibility of using DLP printing to construct elastic GelMA-based vascular scaffolds with high structural precision. The single-component GelMA matrix provided sufficient mechanical strength and elasticity to support complex tubular geometries while remaining compatible with cell culture environments [18]. Compared with extrusion-based methods, the DLP approach offered smoother lumen surfaces and higher reproducibility, which are crucial for achieving uniform shear stress and promoting endothelial cell alignment in subsequent perfusion studies [19]. The successful fabrication of both Y-shaped and curved forms demonstrates the tunability of the printing process and establishes a robust platform for designing microvascular networks that closely mimic natural blood vessel morphology [20].

The data in Figure 3 demonstrate that the DLP-printed GelMA scaffolds possess both high elasticity and mechanical stability, key prerequisites for vascular-mimetic applications. The J-shaped tensile response confirms the intrinsic resilience of the crosslinked GelMA network, which allows energy dissipation and recovery similar to natural soft tissues [21]. Meanwhile, the strong compressive performance highlights the structural continuity and uniform crosslinking achieved through high-resolution photopolymerization [22]. Another important finding of this study is that the printed GelMA scaffolds exhibited mechanical behavior compatible with their intended vascular-mimetic function. As shown by the tensile and compressive curves, the scaffolds displayed nonlinear deformation characteristics and maintained structural stability over a relatively large strain range. This behavior indicates that the crosslinked GelMA network was not excessively brittle after DLP printing, which is critical for tubular constructs that may experience bending, stretching, or localized compression during handling and subsequent application. From the perspective of the present study, the mechanical results do not simply demonstrate that the material is “strong enough”; more importantly, they show that the fabricated scaffolds possess a balance between deformability and integrity, allowing them to better approximate the compliant nature of soft biological conduits. The nonlinear J-shaped tensile response observed in the printed GelMA scaffold is likely associated with the progressive recruitment of the crosslinked polymer network during deformation. At relatively low strain, the hydrogel network can deform through chain rearrangement, local segment rotation, and partial straightening of initially relaxed polymer chains, resulting in a comparatively low apparent stiffness. As the strain increases, a larger

fraction of the network becomes stretched and load-bearing, leading to a more rapid rise in stress. This transition from an initially compliant response to strain-dependent stiffening is consistent with the mechanical behavior of many hydrated soft materials and is particularly relevant for vascular-mimetic scaffolds, which are expected to deform under load while still maintaining structural continuity.

Compared with traditionally cast hydrogels, DLP-printed GelMA exhibits more consistent mechanical profiles due to precise control of curing depth and network homogeneity [23]. These properties ensure that the printed scaffolds can sustain fluid flow and mechanical deformation encountered in perfusion or implantation environments, providing a mechanically reliable platform for subsequent biological evaluation [24].

The results in Figure 4 highlight that the DLP-printed GelMA scaffolds are highly biocompatible and favorable for cell attachment and proliferation. The high viability values obtained from the CCK-8 assay confirm that the printing and post-curing process did not leave cytotoxic residues, which is essential for further biointegration [25]. The live/dead imaging supports that the smooth inner lumen and the presence of natural gelatin-derived RGD motifs facilitate cellular adhesion and survival.

Moreover, the observed cell alignment along the lumen direction implies that the scaffold's cylindrical structure provides topographical cues that may promote endothelial orientation under flow conditions [26]. This structural guidance, combined with the hydrogel's mild mechanical compliance, could play a key role in future applications such as endothelialization of vascular grafts or microfluidic co-culture systems [27]. The preferential arrangement of cells along the lumen is also mechanistically meaningful rather than being merely a visual observation. One possible explanation is the topological guidance provided by the cylindrical inner surface of the scaffold. Unlike a flat substrate, the tubular geometry imposes directional spatial confinement, which can bias the extension and adhesion of cells along the longitudinal axis of the lumen. In this context, the local curvature of the scaffold surface may influence cytoskeletal organization and focal adhesion distribution, thereby favoring an elongated morphology aligned with the available adhesive direction. Overall, these results establish the printed GelMA scaffold as a promising platform for vascularized tissue constructs.

The conceptual framework shown in Figure 5 emphasizes the translational potential of DLP-printed GelMA vascular scaffolds beyond simple structural replication [28]. By integrating microfluidic design and cell mechanobiology, these constructs can bridge the gap between engineered hydrogels and functional vascular tissues [29]. The ability to impose controlled shear stress enables studies of cell alignment, permeability, and endothelial barrier formation—key parameters for vascular physiology modeling [30].

In addition, the compatibility of GelMA with other biomaterials and bioinks allows hybrid fabrication for *in vitro* organ-on-chip platforms [31,32]. These devices can model tissue–vascular interactions under realistic flow, paving the way for applications in drug screening, disease modeling, and personalized medicine [33]. Overall, this figure envisions a progression from static biocompatible scaffolds toward dynamic, perfusable systems capable of emulating real vascular function in engineered tissues.

Overall, the discussion of the present results should be centered on the fact that the fabricated GelMA scaffolds successfully integrated three key requirements of vascular-mimetic constructs, namely controlled hollow architecture, elastic mechanical response, and favorable cytocompatibility. These findings distinguish the present study from a simple printing demonstration and support its relevance for subsequent vascularized tissue engineering applications.

5. Conclusion

In summary, this study established a DLP-based strategy for the fabrication of vascular-mimetic GelMA tubular scaffolds with controlled lumen geometry, elastic mechanical behavior, and favorable cytocompatibility. By introducing 0.02% (w/v) tartrazine as a light-absorbing agent, the printing process achieved improved curing-depth control, which contributed to enhanced lumen fidelity and structural integrity in the printed constructs. The resulting scaffolds successfully reproduced representative

vascular-like geometries and supported cell survival and attachment on the tubular interface. Beyond demonstrating the feasibility of fabricating such structures, the present work suggests that these scaffolds may serve as promising candidate platforms for future applications in microvascular regeneration, perfusable tissue models, and organ-on-chip systems. Their well-defined hollow architecture and compliant mechanical response make them particularly attractive for studies involving cell–flow interaction, endothelialization, and biomimetic microenvironment design. Future work should focus on evaluating the scaffolds under long-term perfusion conditions, promoting functional endothelial lining on the lumen surface, and validating their performance in more physiologically relevant *in vitro* or *in vivo* models. These efforts will help further clarify the practical potential of the present system in vascularized tissue engineering and microphysiological applications.

Acknowledgement: Not applicable.

Funding Statement: The authors declare that they have received no funding. The study was supported by Hunan Provincial Natural Science Foundation of China (2023JJ50220).

Author Contributions: All authors contributed to this present work: Xiaotian Zhang and Kai Li designed the study. Li Yang acquired and interpreted the data. Suyin Feng drafted the manuscript. Runfeng Sun revised the manuscript. All authors reviewed and approved the final version of the manuscript.

Availability of Data and Materials: The datasets generated and/or analyzed during the current study are available from the corresponding author Li Yang upon reasonable request.

Ethics Approval: Ethical approval was not required for this study because it is not involved any human experiments.

Conflicts of Interest: The authors declare no conflicts of interest.

Consent for Publication: Not applicable.

Abbreviations

3D	Three-dimensional
DLP	Digital light processing
GelMA	Gelatin methacryloyl
PBS	Phosphate-buffered saline

References

1. Bahrami N, Haramshahi SMA, Jamali SA, Saeed M, Pezeshki-Modaress M. Biocomposite microfibrous/hydrogel scaffold containing sulfated alginate hydrogel for acceleration of chondrogenic differentiation. Mater Des. 2025;256:114259. doi:10.1016/j.matdes.2025.114259.
2. Calistri S, Ciantelli C, Cataldo S, Cuzzola V, Guzzinati R, Busi S, et al. Simple spin-coating preparation of hydrogel and nanoparticle-loaded hydrogel thin films. Coatings. 2025;15(7):859. doi:10.3390/coatings15070859.
3. Blessing E, Antaredja M, Tilemann L, Oberacker R. Implantation of vascular mimetic implants in challenging chronic total occlusions–Supera™ Extreme. Vasa. 2021;50(6):475–9. doi:10.1024/0301-1526/a000918.
4. Da Silva André G, Paganella LG, Badolato A, Sander S, Giampietro C, Tibbitt MW, et al. Protein isolation from 3D hydrogel scaffolds. Curr Protoc. 2024;4(1):e966. doi:10.1002/cpz1.966.
5. Chen C, Wu D, Wang Z, Liu L, He J, Li J, et al. Peptide-based hydrogel scaffold facilitates articular cartilage damage repair. ACS Appl Mater Interfaces. 2024;16(9):11336–48. doi:10.1021/acsami.4c00811.

6. Chen J, Gui X, Qiu T, Lv Y, Fan Y, Zhang X, et al. DLP 3D printing of high-resolution root scaffold with bionic bioactivity and biomechanics for personalized bio-root regeneration. Biomater Adv. 2023;151(1):213475. doi:10.1016/j.bioadv.2023.213475.
7. Francis RM, DeForest CA. 4D biochemical photocustomization of hydrogel scaffolds for biomimetic tissue engineering. Acc Mater Res. 2023;4(8):704–15. doi:10.1021/accountsmr.3c00062.
8. Du Y, Hu T, You J, Ye Y, Zhang B, Bao B, et al. Study of falling-down-type DLP 3D printing technology for high-resolution hydroxyapatite scaffolds. Int J Appl Ceram Technol. 2022;19(1):268–80. doi:10.1111/ijac.13915.
9. Cheng J, Xue J, Yang Y, Yu D, Liu Z, Li Z. Hierarchical hydrogel scaffolds with a clustered and oriented structure. J Mater Chem B. 2023;11(21):4703–14. doi:10.1039/d3tb00497j.
10. Gao X, Yang J, Gan X, Lin Y, Xu J, Shan Z, et al. Optimized DLP 3D-printed high-resolution nano zirconia-hydroxyapatite scaffold with craniomaxillofacial soft tissue invasion resistance and pro-osteogenic properties via dectin-1/syk inflammatory axis. Chem Eng J. 2024;491(1):152044. doi:10.1016/j.cej.2024.152044.
11. Guo Y, Mou S, Suo L, Zhou Y, Wu S, Xie X, et al. Porous granular hydrogel scaffolds biofabricated from dual-crosslinked hydrogel microparticles for breast tissue engineering. Mater Today Bio. 2025;33:102006. doi:10.1016/j.mtbio.2025.102006.
12. Han S, Liang W, Wan H, Tian L, Wen C, Wu Q, et al. Vascular-mimetic 2D membranes with hemoglobin catalysis for efficient uranium extraction. Adv Mater. 2026;38(1):e09989. doi:10.1002/adma.202509989.
13. Jaberi A, Ghelich P, Samandari M, Kheirabadi S, Ataie Z, Kedzierski A, et al. Gelatin methacryloyl granular hydrogel scaffolds for skin wound healing. Biomater Sci. 2025;13(21):6013–23. doi:10.1039/d4bm01062k.
14. He Z, He S. Two-photon polymerization of hydrogel cellular scaffolds. Opt Commun. 2025;574:131161. doi:10.1016/j.optcom.2024.131161.
15. Jaberi A, Xiang Y, Sheikhi A. Multiscale structure-property relationships in gelatin-based granular hydrogel scaffolds. ACS Macro Lett. 2025;14(10):1569–78. doi:10.1021/acsmacrolett.5c00441.
16. Jamali SA, Mohammadi M, Saeed M, Haramshahi SMA, Shahmahmoudi Z, Pezeshki-Modaress M. Biomimetic fiber/hydrogel composite scaffolds based on chitosan hydrogel and surface modified PCL chopped-microfibers. Int J Biol Macromol. 2024;278:134936. doi:10.1016/j.ijbiomac.2024.134936.
17. Kashyap S, Mohanty S, Sen S, Roy S. Designing an entactin-inspired short bioactive hydrogel as biofunctional scaffold. ChemBioChem. 2025;26(14):e202500260. doi:10.1002/cbic.202500260.
18. Ali Mohammad Khani A, Barati Haghverdi A, Rezaei I, Soldoozy A, Aghaee T. Hydrogel-based THz wave absorber. Results Opt. 2025;19:100810. doi:10.1016/j.rio.2025.100810.
19. Liang J, Huang X, Qin K, Wei H, Yang J, Liu B, et al. Implanted magnetoelectric bionic cartilage hydrogel. Adv Mater. 2025;37(20):2415417. doi:10.1002/adma.202415417.
20. Lazarenko MM, Zabashta YF, Honcharuk DK, Alekseev OM, Yablochkova KS, Vergun LY, et al. Determining hydrogel porosity through dielectric relaxation intensity ratios between water and hydrogel. Soft Matter. 2025;21(21):4298–305. doi:10.1039/d5sm00077g.
21. Lin CL, Liu JT, Shin CS. High-resolution DLP 3D printing for complex curved and thin-walled structures at practical scale: archimedes microscrew. Micromachines. 2025;16(7):762. doi:10.3390/mi16070762.
22. Ma J, Zhang X, Xu Y, Wang W, Zhu T, Cai J. Construction of hydroxyapatite gradient hydrogel scaffolds by electrodeposition. ACS Appl Bio Mater. 2025;8(10):9299–309. doi:10.1021/acsabm.5c01427.

23. Nandan V, Ramswamy CA, Gowda SS, Desai SC, Neeli DKS, Kumar V. Outcomes and patency of vascular mimetic stents in long-segment femoral artery lesions. Indian J Vasc Endovasc Surg. 2025;12(1):14–8. doi:10.4103/ijves.ijves_98_24.
24. Mohammad Mehdipour N, Rajeev A, Kumar H, Kim K, Shor RJ, Natale G. Anisotropic hydrogel scaffold by flow-induced stereolithography 3D printing technique. Biomater Adv. 2024;161(1):213885. doi:10.1016/j.bioadv.2024.213885.
25. Pan J, Yang Z, Chen HR, Yan B, Li HX, Ke Y, et al. Thermoresponsive hydrogel with thermal memory. Adv Mater. 2026;38(2):e11341. doi:10.1002/adma.202511341.
26. Zhao C, Zhou S, Ma J, Liu C, Zhu J, Ye S, et al. Highly conductive PANI/ATMP/$AgNO_3$ composite hydrogel electrodes for all-hydrogel-state supercapacitors. J Mater Chem A. 2025;13(7):5238–51. doi:10.1039/d4ta07437h/v2/review1.
27. Su P, Hu Y, Li J, Wei D, Fu W. Biodegradable PHBVHHx-PEG/collagen hydrogel scaffolds for cartilage repair. Tissue Eng Part A. 2025;31(15–16):1039–50. doi:10.1089/ten.tea.2024.0108.
28. Ye X, Qin K, Yang R, Dijksman JA. Rebounding hydrogel sphere water entry. J Fluid Mech. 2025;1013:A2. doi:10.1017/jfm.2025.10207.
29. Tian H, Zhou R, Ke L, Qian K, Liu Y, Hao J. A mechanically durable hydrogel synapse. Adv Funct Mater. 2025;35(34):2505232. doi:10.1002/adfm.202505232.
30. Wang C, Zhou Y. Cast-molded channelized hydrogel scaffolds with stereolithography-printed templates. Biotechnol Bioeng. 2025;122(10):2874–87. doi:10.1002/bit.70007.
31. Xin Z, Wang A. A novel recyclable anti-fatigue hydrogel: polyvinyl alcohol/glycerol/bamboo microfibril double-network hydrogel. Adv Eng Mater. 2025;27(22):e202501065. doi:10.1002/adem.202501065.
32. Yan X, Yang Z, Ma A, Chen Z, Wang Y. AB-type zwitterionic hydrogel paint. Langmuir. 2025;41(2):1519–25. doi:10.1021/acs.langmuir.4c04857.
33. Xu F, Jin H, Wu H, Jiang A, Qiu B, Liu L, et al. Digital light processing printed hydrogel scaffolds with adjustable modulus. Sci Rep. 2024;14(1):15695. doi:10.1038/s41598-024-66507-x.

Received: 10 November 2025; Accepted: 07 April 2026; Published: XX XX 2026